Inception of a Devonian subduction zone along the southwestern Gondwana margin: ^{40}Ar–^{39}Ar dating of eclogite–amphibolite assemblages in blueschist boulders from the Coastal Range of Chile (41°S)

Terence T. Kato, Warren D. Sharp, and Estanislao Godoy

Abstract: Coarsely crystalline residual blueschist boulders from the Coastal Range of south-central Chile (41°S) contain relict eclogite–amphibolite assemblages that provide evidence of pre-Carboniferous high pressure relative to temperature (high *P*/*T*) metamorphism along the southwestern continental margin of Gondwana. Early assemblages in the exotic boulders include omphacite, garnet, and hornblende that indicate eclogite-facies conditions of $T = 553 \pm 30$ °C and $P > 1.32 \pm 0.04$ GPa during metamorphism, corresponding to a low geothermal gradient of <12.5 °C/km. These phases are replaced to varying degrees by sodic amphibole + epidote assemblages. Relict hornblende from an early garnet amphibolite assemblage within blueschist yields an ^{40}Ar–^{39}Ar plateau age of 361 ± 1.7 Ma, providing a minimum age for early high *P*/*T* metamorphism. Coarse white micas that partially replace the hornblende and are in textural equilibrium with glaucophane yield plateau and near-plateau ages of 325 ± 1.1 Ma and ~320 Ma, respectively. We interpret these data to indicate that late Paleozoic high *P*/*T* metamorphism related to subduction of oceanic lithosphere along the southwestern paleo-Pacific margin of Gondwana began prior to 361 Ma (Late Devonian). Subsequent retrograde metamorphism involving fluid infiltration and decreasing thermal gradients resulted in conversion of coarse eclogite–amphibolite to blueschist by ~325 Ma in the dated samples.

Résumé : Des blocs résiduels de schistes bleus à gros cristaux de la chaîne côtière du centre-sud du Chili (41°S) contiennent des assemblages reliques éclogite – amphibolite qui fournissent des évidences de métamorphisme à haute pression à température (*P*/*T* élevées) le long de la bordure sud-ouest du continent de Gondwana au pré-Carbonifère. Des assemblages précoces dans les blocs exotiques comprennent de l'omphazite, du grenat et de la hornblende qui signalent un faciès éclogite dont les conditions de température et de pression étaient respectivement de 553 ± 30 °C et > 1,32 ± 0,04 GPa durant le métamorphisme, correspondant à un faible gradient géothermique, < 12,5 °C/km. À divers degrés, ces phases sont remplacées par des assemblages amphibole sodique + épidote. De la hornblende relique d'un assemblage précoce de grenat amphibolite dans le schiste bleu a donné un âge ^{40}Ar–^{39}Ar plateau de 361 ± 1,7 Ma, fournissant un âge minimum pour le métamorphisme précoce à *P*/*T* élevées. Des micas blancs grossiers qui remplacent en partie la hornblende et qui sont en équilibre textural avec le glaucophane ont des âges plateau et proche plateau respectifs de 325 ± 1,1 et ~320 Ma. Selon nous, ces données indiquent que le métamorphisme à *P*/*T* élevées au Paléozoïque tardif, et relié à la subduction de la lithosphère océanique le long de la bordure sud-ouest paléo-Pacifique de Gondwana, a débuté avant 361 Ma (Dévonien tardif). Un métamorphisme rétrograde subséquent impliquant une infiltration de fluides et des gradients thermiques décroissants a résulté en la conversion de l'assemblage grossier éclogite – amphibolite en schiste bleu vers ~325 Ma dans les échantillons datés.

[Traduit par la Rédaction]

Introduction

The assembly of the southwestern pre-Andean (Gondwana) margin of western South America is generally considered to record a prolonged history of terrane accretion extending into the late Paleozoic (Ramos et al. 1986; Mpodozis and Kay 1992). Subduction along the Gondwana margin as early as the middle Ordovician is inferred from magmatic, structural deformational, and stratigraphic criteria (Bahlburg and Hervé 1997). High pressure–temperature (*P*–*T*) subduction-related metamorphism related to pre-Carboniferous accretion, however, is not reported, even between large Paleozoic terranes, such as the Chilenia, Precordillera, Pampeanas, and Patagonia, that compose much of the northern Patagonia

Received 5 September 2007. Accepted 1 February 2008. Published on the NRC Research Press Web site at cjes.nrc.ca on 23 April 2008.

Paper handled by Associate Editor W.J. Davis.

T.T. Kato.[1] Department of Geological and Environmental Sciences, California State University, Chico, CA 95929 USA.
W.D. Sharp. Berkeley Geochronology Center, 2455 Ridge Rd, Berkeley, CA 94709, USA.
E. Godoy. Servicio Nacional de Geología y Minería de Chile, Casilla 104605, Santiago, Chile.

[1]Corresponding author (e-mail: tkato@csuchico.edu).

 doi:10.1139/E08-006

Fig. 1. Regional map showing distribution of basement complexes of Chile and Argentina between latitudes 34°S and 43°S (map modified from Cingolani et al. 1991). Inset map A is the northern extension of the main map area.

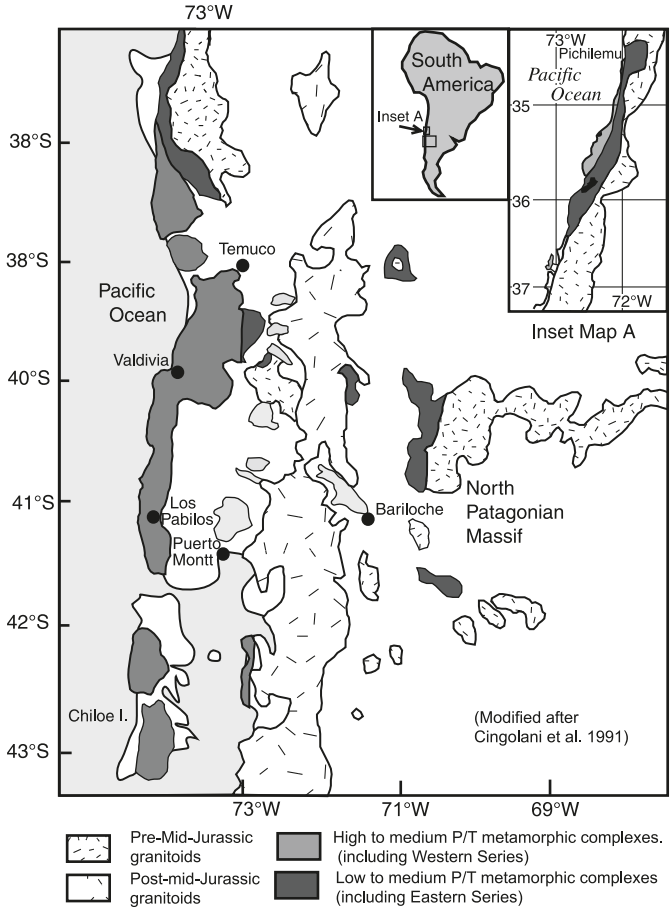

portion of Gondwana. One of the few complexes in which blueschist minerals occur is in the Western Series of south-central Chile (Fig. 1) (Aguirre et al. 1972). This subduction complex occupies a position external to accreted Gondwana terranes and the coeval North Patagonian magmatic arc (Hervé et al. 1988; Martin et al. 1999). In northern Chile, the western margin of Gondwana is considered to have been a passive margin from the early Silurian to the late Carboniferous (Bahlburg and Hervé 1997). In contrast, the data presented in this paper suggest that in south-central Chile, ocean–continent convergence, and thus an active margin, was established along the pre-Andean, paleo-Pacific continental margin of southwestern Gondwana by the Late Devonian.[2]

Petrographic, electron microprobe mineral analyses, and ^{40}Ar–^{39}Ar dating evidence are presented for selected boulders of coarse crystalline blueschists (retro-eclogite–amphibolite) from the Coastal Range of South Central Chile in the Los Pabilos area (41°S) to establish a date for inception of high *P*/*T* metamorphism, describe the formation of eclogite and amphibolite remnants in coarse blueschist, and explain how the older, less deformed, and higher grade, exotic blocks attained their superjacent position relative to the in situ Western Series schist. These blocks are not observed in place within the underlying, predominately younger Western Series metamorphic complex; however, we will present evidence that the exotic blocks described here may have constituted an older, more deeply subducted, volumetrically minor protolith within the regional subduction complex.

Coarsely crystalline high-grade blueschists containing relict amphibolite–eclogite lithologies somewhat similar to the Los Pabilos boulders, occur in the California Coast Range, where they comprise an older, higher grade, anomalous constituent of the Franciscan subduction complex (Coleman and Lee 1963; Ernst et al. 1970; Cloos 1986; Wakabayashi 1990; Tsujimori et al. 2006). High-grade blueschists after earlier eclogite–amphibolite protoliths also occur as older constituents of many other subduction complexes, where they often record complex and varied exhumation histories (e.g., Baldwin 1996; Carson et al. 2000).

Regional Geologic setting

Fragmented and laterally transposed remnants of a late Paleozoic subduction complex and magmatic arc are widely distributed throughout the Chilean Coastal Range and Western Andes south of 35°S (Hervé et al. 1981) (Fig. 1). This complex, the "crystalline basement" (González-Bonorino 1970), contains both the exhumed remnants of a high *P*/*T* subduction complex, the "Western Series" (WS), and a low *P*/*T*, less penetratively deformed "Eastern Series" (ES) (Aguirre et al. 1972; Hervé et al. 1974; Ernst 1975). Sodic amphiboles were first recognized in coastal exposures of the WS near the town of Pichilemu (34°20′S) (Hervé et al. 1974). Although thought to be largely composed of late Paleozoic constituents (Martin et al. 1999; Duhart et al. 2001), in the Andean foothills (42°S), sparse Devonian trilobite fossils (Fosiles de Buill) are associated with the ES metasediments (Fortey et al. 1992). The WS–ES-type subdivision continues at least as far south as the Chonos Archipelago (47°S) (Godoy et al. 1984; Willner et al. 2000).

The Bahía Mansa Metamorphic Complex (BMMC) (Duhart et al. 2001), the portion of the WS that comprises most of the Chilean Coast Range between 38°S and 42°S latitudes, is composed mainly of quartz–mica schist of clastic origin and subordinate mafic schist (metabasalt) and metachert (Kato 1976, 1985). The regional distribution of mafic schist-rich zones during the regional mapping of the BMMC (Duhart et al. 2001) is shown in Fig. 2*a* along with representative S_2 attitudes formed during later D_3 folding and thrust faulting (Martin et al. 1999). The BMMC is characterized by distinct planar schistosity and ubiquitous greenschist mineral assemblages, which largely obscure earlier non-greenschist assemblages (Kato 1985; Martin et al. 1999; Duhart et al. 2001).

High pressure relative to temperature (high *P*/*T*) phases identified within this portion of the WS include lawsonite

[2] Supplementary data are also available. Table S1: $^{40}Ar/^{39}Ar$ analytical data. Table S2: electron microprobe analyses of minerals. Supplementary data can be found on the journal Web site (http://cjes.nrc.ca) or may be purchased from the Depository of Unpublished Data, Document Delivery, CISTI, National Research Council of Canada, Building M-55, 1200 Montreal Road, Ottawa, ON K1A 0R6, Canada. For more information on obtaining material, refer to http://cisti-icist.nrc-cnrc.gc.ca/irm/unpub_e.shtml.

Fig. 2. Map representations of (A) Bahia Mansa Metamorphic Complex (BMMC) portion of Western Series complex lithologic distribution (modified from Duhart et al. 2001). (B) Total magnetic field intensity map. Grayscale rendition of Carta Magnetica de Chile, 1980 (Courtesy G. Yañez). (C) Detail of sample area of the Cuesta Brava serpentinite west of Los Pabilos (Geology modified from Kato and Godoy 1995). Cret., Cretaceous; Qtz, quartz; UTM, Universal Transverse Mercator.

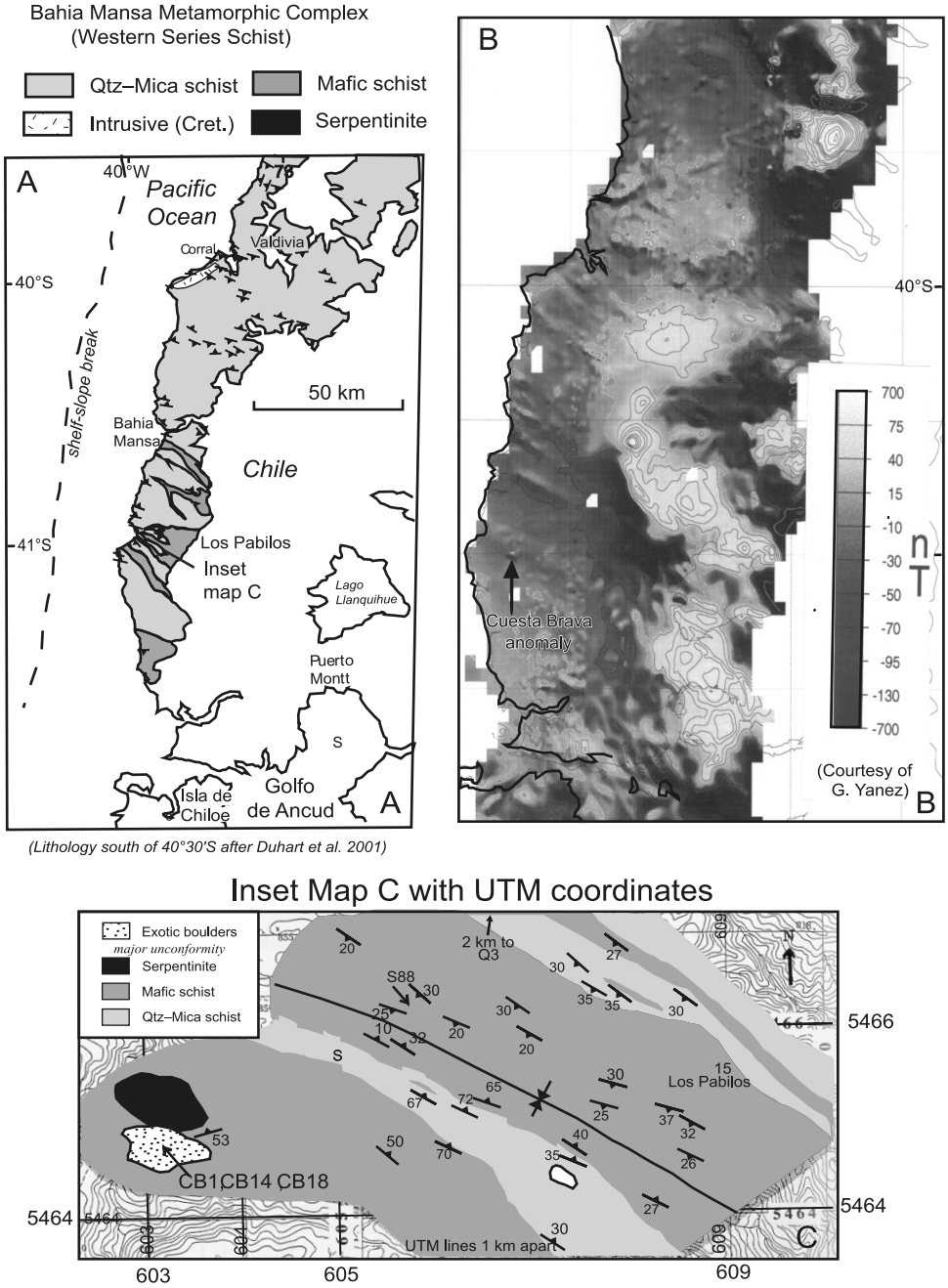

(Saliot 1969) and glaucophane in metapelites on Chiloé Island (42°30′S) (Kato 1976) and relict sodic amphibole from in situ schists in the area between Valdivia and Puerto Montt (40°S–41°S) (Kato et al. 1997; Martin et al. 1999; Duhart et al. 2001). Minerals often associated with high *P*/*T* conditions, such as stilpnomelane (Aguirre et al. 1972) and zussmanite (Massonne et al. 1998) are also reported. Various intermediate Ca–Na amphiboles of the barroisite–winchite series and highly phengitic white micas are common in the complex and suggest peak pressures of 0.7–0.99 GPa within primarily greenschist assemblages (Willner et al. 2001). Biotite and garnet, suggesting early higher temperatures are also common as relict mineral phases in the lower greenschist assemblage, suggesting higher grade earlier metamorphic conditions in the northeastern portion of the BMMC (Kato 1985).

Exotic blueschist (retro-eclogite–amphibolite) boulders from Los Pabilos

Location and Setting

In contrast to the well-foliated schistose BMMC outcrops,

Fig. 3. Photomicrographs: (A) Sample CB 14: retro-eclogite exotic boulder, showing general mineral content contrasting early (garnet + omphacite + hornblende) and late (sodic amphibole + epidote + white mica) assemblages. (B) Sample CB 14: local replacement of omphacite by hornblende. (C) Sample S88: in situ mafic schist (with relict hornblende). (D) Sample Q3: in situ mafic schist (with relict sodic amphibole). hb, hornblende; na, sodic amphibole; ca, calcic to calci-sodic amphibole; ep, epidote; wm, phengitic muscovite; gt, garnet; om, omphacitic pyroxene; stp, stilpnomelane; sph, sphene; mag, magnetite.

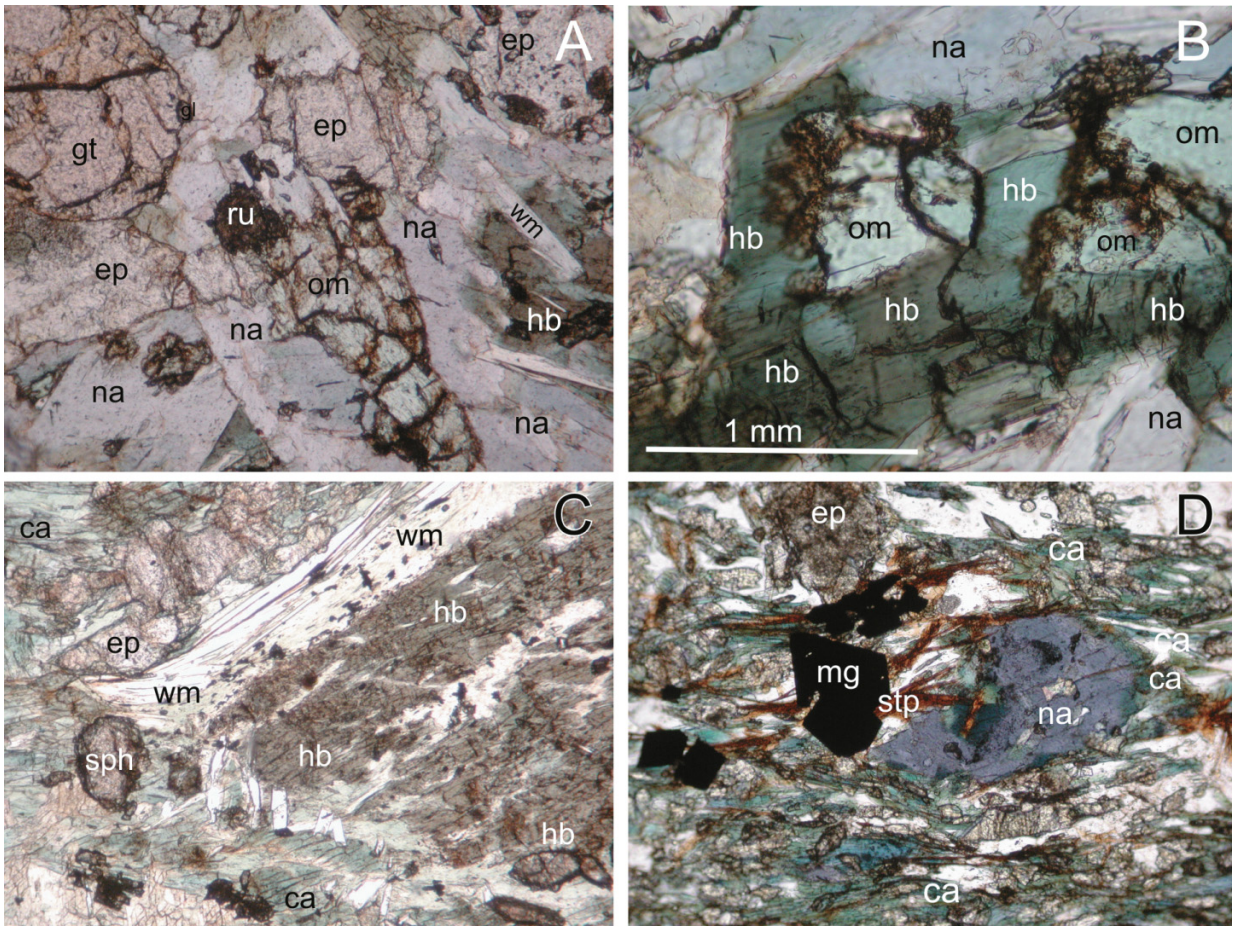

anomalous coarsely crystalline, sodic amphibole–epidote blueschists, retro-amphibolite, and retro-eclogite occur in the south-central Coast Range as surficial rounded boulders and mudflow deposits near the lumber camp of Los Pabilos (41°S) (Kato 1976, 1985; Kato and Godoy 1995). Although relict hornblende-bearing epidote and garnet amphibolites have been described in these boulders (Kato 1976; Kato and Godoy 1995; Willner et al. 2004), we present here the first report of remnant omphacite + garnet, indicating the earlier presence of eclogite. This association also allows us to estimate metamorphic temperature and minimum pressure of the eclogite protolith by Fe–Mg exchange equilibria and net transfer reactions.

The boulders partially rest upon a distinctive 1 km^2 serpentinite mass within the in situ BMMC west of Los Pabilos, in an area referred to locally as Cuesta Brava. The Cr-magnetite-rich serpentinite forms a circular ±100 nT magnetic anomaly at 40°57′S, 73°47′W on the 1 : 100 000 scale magnetic map of Chile (1980). On the regional aeromagnetic compilation map (Fig. 2*b*) many of the small localized anomalies are serpentinite, whereas the longer more linear anomalies are due to dipping magnetite-bearing mafic schist (S_2) layers (Godoy and Kato 1990). Large (>1.0 m) boulders of the underlying serpentinite and in situ mafic schist are intermixed with the blueschist boulders, suggesting that they were all associated within the complex prior to being eroded and deposited on the surface. Samples of the exotic boulders (see Fig. 2*a*) and in situ schists from the local area, exceeding 100 in number, were examined in hand specimen and in thin section.

Lithologic characteristics of the exotic boulders

The Los Pabilos exotic boulders, unlike the in situ mafic schists, often contain sodic amphiboles (glaucophane) as part of the latest phase assemblage replacing earlier eclogite–amphibolite assemblages, including hornblende, garnet, and omphacite (Fig. 3*a*). The coarse blueschist assemblages in most samples lack foliation and have not been replaced by later more calcic amphiboles. In sample CB 14, a retro-eclogite blueschist sample, the only one containing relict omphacite, garnet, and hornblende, appears to be in textural equilibrium, although in rare instances hornblende surrounds and partially replaces the omphacite (Fig. 3*b*). The relatively unfoliated coarse blueschist of the exotic boulders contrasts with the well foliated, finer grained, in situ, greenschist-

Fig. 4. Sample CB14: Retro-eclogite. Photomicrograph (A) and backscattered electron (B) images of relict omphacitic pyroxene. Omphacite (om) shown in various stages of replacement in sample by blueschist assemblage containing glaucophane (gl), epidote (ep), albite (ab), and sphene (sph). Note calcium-rich (lighter) domains in BSE image of pyroxene. Calcic amphibole (ca) present as latest stage replacement of both omphacite and glaucophane. Ca amphibole growth forms incipient S_2 foliation.

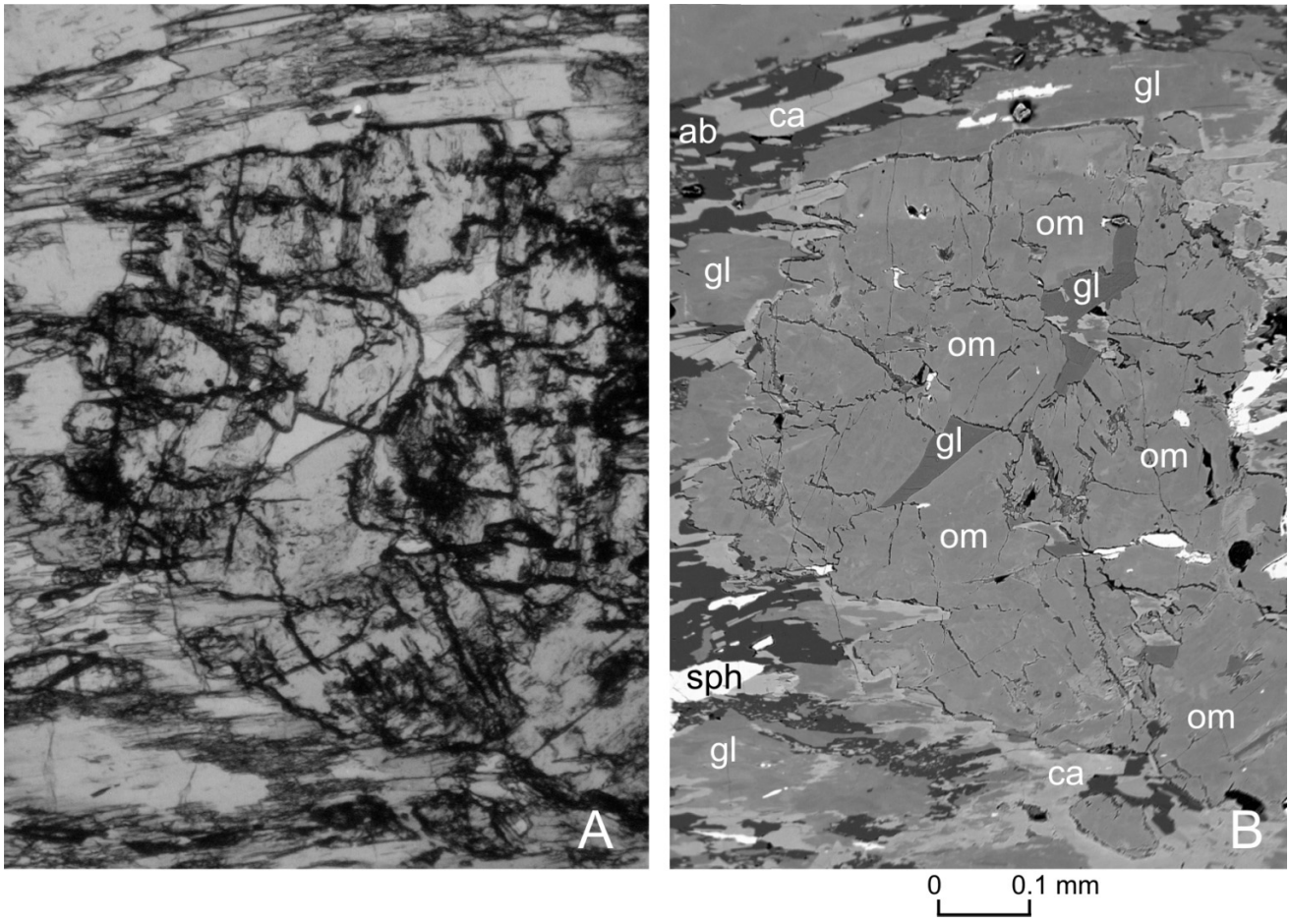

grade mafic schist (Figs. 3*c*, 3*d*). Fine, incipient crystals of syn-folial Ca amphibole, however, are present in some of the samples forming a crude, incipient, latest stage foliation on pre-existing more randomly oriented blueschist mineral assemblages. This incipient foliation we believe to be related to the S_2 planar fabric characteristic of the in situ BMMC accretionary complex.

In the retro-eclogite sample (CB 14), the earlier omphacite + garnet + hornblende assemblage is replaced by a glaucophane + epidote + white mica assemblage, which in turn is partially replaced by a fine greenschist assemblage with incipient growth of syn-folial calcic amphiboles (actinolites) similar to those in the in situ BMMC greenschists. This is shown in corresponding optical (Fig. 4*a*) and backscattered electron (BSE) (Fig. 4*b*) images.

The compositional ranges of the omphacite and garnet in sample CB 14 are shown in partial triangular diagrams (Fig. 5*a*). Omphacite displays high variability between Ca-rich (Di + He) and sodic rich (Jd + Ac) varieties, which appear to coexist texturally in the sample (Fig. 5*a*). Compositions of the latest stage Ca amphibole (actinolite) are also shown on the diagram. Garnet compositions (Fig. 5*b*) exhibit a distinct difference between the main unzoned (higher pyrope) garnet, believed to have formed in the eclogite assemblage, and a narrow discontinuous rim phase garnet, related to the later blueschist assemblage.

Relict hornblende and sodic amphibole in the in situ Western Series mafic schists

Amphiboles which differ from the actinolite in the regional mafic schist are common in the exotic boulders and are poorly preserved, but widespread in the in situ mafic schists, indicating a wide range of pre-greenschist *P–T* conditions. Compositions from two informative specimens of in situ mafic schist containing anomalous relict minerals are plotted in Fig. 5*c* and listed in Table 1. Large relict hornblende crystals (sample S88, Fig. 3*c*) and sodic amphibole (sample Q3, Fig. 3D) from in situ mafic schists of the BMMC in the Los Pabilos area are compared to those from the exotic blueschist (retro-eclogite) boulder (sample CB14). Relict hornblendes (Al^{IV} = 1.5) from both samples are similar in optical and chemical properties. Sodic amphiboles are present in both the exotic boulders and in sample Q3. Although not represented in the diagram, the sodic amphibole has higher Fe^{3+}/Al^{VI} in sample S88 than in sample CB 14, where Fe^{3+} is calculated on the basis of 46 total charge and cations (Na + Ca + K) = 13 (Papike et al. 1974). The relict sodic amphibole is rarely preserved in the in situ mafic

Table 1. Electron microprobe analyses of representative minerals.

(A)	Sample CB 14 omphacitic pyroxenes							Sample CB 14 garnets					
	Cpx (disord)			Cpx (ord)				Garnet core			Garnet rim		
	pxA3-1	Avg(12)	σ	px3-3	Avg(13)	σ		Gar-C8	Avg(11)	σ	Gar-R10	Avg(9)	σ
Major oxides (wt.%)													
SiO_2	53.69	53.51	0.5	54.42	54.58	0.41		38.03	37.95	0.19	37.67	37.55	0.15
TiO_2	0	0.06	0.04	0.1	0.05	0.03		0.11	0.09	0.04	0.12	0.12	0.04
Al_2O_3	6.08	6.01	1.27	11.98	11.44	0.87		21.58	21.59	0.21	21.67	21.57	0.11
Cr_2O_3	0.02	0.18	0.14	0	0.04	0.02		0.06	0.09	0.09	0.03	0.04	0.03
Fe_2O_3(c)	6.1	6.18	0.6	4.09	3.83	0.55		n.d.	n.d.		n.d.	n.d.	
FeO(c)	2.46	2.3	0.36	2.35	2.81	0.76		23.66	23.7	0.5	20.65	20.8	0.43
MnO	0.17	0.23	0.04	0.16	0.17	0.06		3.48	3.49	0.2	6.7	6.5	0.44
MgO	10.47	10.38	0.81	7.2	7.31	0.53		4.08	3.98	0.17	0.83	0.83	0.1
CaO	17.23	17.56	1.18	11.96	12.85	0.9		10.03	9.92	0.29	13.1	13.4	0.62
Na_2O	4.49	4.42	0.73	7.44	7.08	0.41		n.d.	n.d.		n.d.	n.d.	
Sum oxides	100.72	100.67	0.32	99.7	100.17	0.85		101.03	100.8	0.3	100.8	100.82	0.27
Cations													
Si	1.944	1.94	0.01	1.948	1.95	0.01	Fe	1.54	1.57	0.03	1.36	1.37	0.03
Ti	0	0	0	0	0	0	Mg	0.48	0.46	0.02	0.1	0.08	0.01
Al/Al^{IV}	0.056	0.06	0.01	0.05	0.05	0.01	Mn	0.23	0.22	0.01	0.45	0.44	0.03
Al^{VI}	0.204	0.2	0.07	0.45	0.44	0.02	Ca	0.84	0.81	0.03	1.11	1.13	0.05
Cr	0.001	0	0	0	0	0	Ti	0.01	0	0	0.01	0.01	0
Fe^{3+}	0.166	0.17	0.03	0.11	0.1	0.01	Al	1.98	1.99	0.02	2.02	2.01	0.01
Fe^{2+}	0.075	0.07	0.02	0.07	0.08	0	Si	2.96	2.97	0.01	2.97	2.97	0.01
Mn^{2+}	0.005	0.01	0	0.01	0.01	0	Cr	0	0	0	0	0	0
Mg	0.565	0.56	0.05	0.38	0.38	0.02	SumCat	8.04	8.03	0.01	8.01	8.02	0.01
Ca	0.669	0.68	0.05	0.46	0.49	0.0221	Alm	0.5	0.51	0.01	0.45	0.45	0.01
Na	0.316	0.31	0.05	0.52	0.5	0.01	Pyr	0.15	0.15	0	0.03	0.03	0
Cations	4.001	4		4	4		Sps	0.07	0.07	0	0.15	0.14	0.01
							Grs	0.27	0.26	0.01	0.37	0.37	0.02

(B)	Sample CB 14 amphiboles						Relict amphiboles from in situ mafic schists					
	Hornblende			Sodic amphibole			S88 hornblende			Q3 sodic amphibole		
	hb1c-2	Avg(6)	σ	na3–2	Avg(6)	σ	Hb Pt23	Avg(12)	σ	na3–2	Avg(16)	σ
Major oxides (wt.%)												
SiO_2	44.43	44.16	0.63	57.01	57.74	0.47	44.85	44.69	0.22	57.07	55.39	1.45
TiO_2	0.96	0.93	0.07	0	0.017	0.03	0.85	0.86	0.03	0.27	0.08	0.09
Al_2O_3	14.37	13.86	0.3	11.13	10.93	0.36	12.18	12.11	0.23	7.84	7.12	0.61
Fe_2O_3(c)	2.36	2.55	0.44	4.07	3.48	0.47	n.d.	n.d.		7.11	9.84	1.35
FeO(c)	10.09	10.37	0.25	7.88	8.49	0.55	11.58	11.56	0.25	12.21	9.38	1.5

Table 1 (*concluded*).

(B)	Sample CB 14 amphiboles						Relict amphiboles from in situ mafic schists					
	Hornblende			Sodic amphibole			S88 hornblende			Q3 sodic amphibole		
	hb1c-2	Avg(6)	σ	na3–2	Avg(6)	σ	Hb Pt23	Avg(12)	σ	na3–2	Avg(16)	σ
MnO	0.24	0.22	0.04	0.26	0.13	0.09	0.27	0.24	0.04	0.16	0.13	0.06
MgO	11.53	11.44	0.38	9.96	9.92	0.25	12.87	13.08	0.26	7.01	8.16	0.66
CaO	10.01	9.95	0.23	1.42	1.2	0.25	10.58	10.62	0.19	0.41	0.62	0.18
Na_2O	3.58	3.63	0.21	6.51	6.67	0.23	3.55	3.34	0.15	6.48	6.45	0.18
K_2O	0.45	0.48	0.04	0.04	0.02	0.02	0.31	0.33	0.03	0	0.08	0.01
H_2O(c)	2.07	1.98	0.12	2.1	2.17	0.04	n.d.	n.d.		2.13	2.07	0.06
Sum oxides	100.12	99.66	0.92	100.48	100.8	0.41	96.39	96.88	0.36	100.71	99.3	1.29

Note: n.d., not detected; ord, ordewred phase; disord, disordered phase; Avg(*n*), average (number of samples), SumCat, sum of cations; Alm, almandine; Pyr, pyrope; Sps, spessartine.

schist, which contains Ca (actinolite) and Na–Ca (winchite–barroisite) amphiboles, but is ubiquitous in the exotic boulders as part of late stage mineral assemblages. Electron microprobe analyses for various minerals mentioned in this paper are listed in Table 1. Due to the extreme variability and questionable stability within the assemblage, analyses for Na–Ca amphiboles are not included.

Evidence for early stage (pre-Carboniferous) high *P/T* metamorphic conditions

The relict mineralogy of the exotic boulders suggests a range of early peak metamorphic conditions. Both the omphacite and hornblende are always surrounded and partially replaced by the late-glaucophane assemblage, suggesting that the relict minerals represent early pre-blueschist conditions ranging from eclogite to epidote-amphibolite-facies conditions. Unaltered contacts between omphacite and garnet indicate textural equilibrium.

The lower and higher jadeite (Jd) portions of the omphacite in BSE images are irregular and may represent initial immiscibility of more and less ordered (higher Na) domains, as suggested in Jd-rich pyroxenes near these *P–T* conditions (Holland 1983). Unlike many eclogites associated with blueschists, where garnet (Gt) commonly shows strong compositional zoning (Ghent 1988), the garnet in sample CB14 is essentially unzoned, except for a narrow Ca-rich outer rim. BSE and X-ray map images confirm the absence of zoning in the main garnet. In general, the garnets from exotic boulders are higher in pyrope component and display far less zoning than in relict garnets from the in situ mafic schists of the BMMC (Kato and Godoy 1995).

An estimate of *P–T* conditions representing probable peak metamorphic conditions is determined by combining the pressure dependent clinopyroxene (Cpx) reaction curve (jadeite(0.5) + quartz = albite) and the geothermometer of Krogh Ravna (2000), based on $K_D = (Fe/Mg)^{Gt}/(Fe/Mg)^{Cpx}$. This geothermometer is considered to be independent of sodium in clinopyroxene in the range of $X^{Cpx}_{Na=0-0.5}$(Krogh Ravna 2000). A minimum pressure is determined by the Jd in Cpx equilibria curves of Holland (1983).

The data for the retro-eclogite CB14 gives approximate conditions of $T = 553 \pm 30$ °C and $P > 1.32 \pm 0.04$ GPa. Quartz is present only as inclusions in garnet; therefore, the pressure estimate is considered a minimum value. Albite ($An_{0.3}$ to $An_{0.5}$) is present in minor quantities in textural equilibrium with glaucophane. Calculation of (Fe^{2+}/Mg) in the exchange reaction was used with Fe^{+3} corrections calculated for clinopyroxene (Fe^{3+} = Na – Al) and in garnet by (Fe^{+3} = 8 – 2S – 2Ti – Al). The average Jd composition of omphacite is used because the more sodic Jd_{50} portion (P2/n ordered phase) of the omphacitic pyroxene appears to be the original phase (darker portion on BSE image, see Fig. 4*a*); whereas the higher Ca cpx domains appear to represent an exsolved or metastable disordered phase (P2/n + C2/c) as noted in other omphacites (Rossi 1988). Problems with application of the type of geothermometer and barometer used here have been discussed in previous studies (e.g., Holland 1983; Ghent 1988; Krogh Ravna 2000).

The conditions thus calculated would correspond to a maximum linear ambient gradient <12.5 °C/km ($\rho \approx 3.05$ g/cm^3), indicating very low-temperature gradient during

Fig. 5. Composition diagrams for (A) clinopyroxene, (B) garnet, and (C) amphibole. Arrows on Fig. 5C show order of formation of amphiboles based on textural zonation. Chemical compositions are summarized in Table 1. ord., ordered phase; disord., disordered phase.

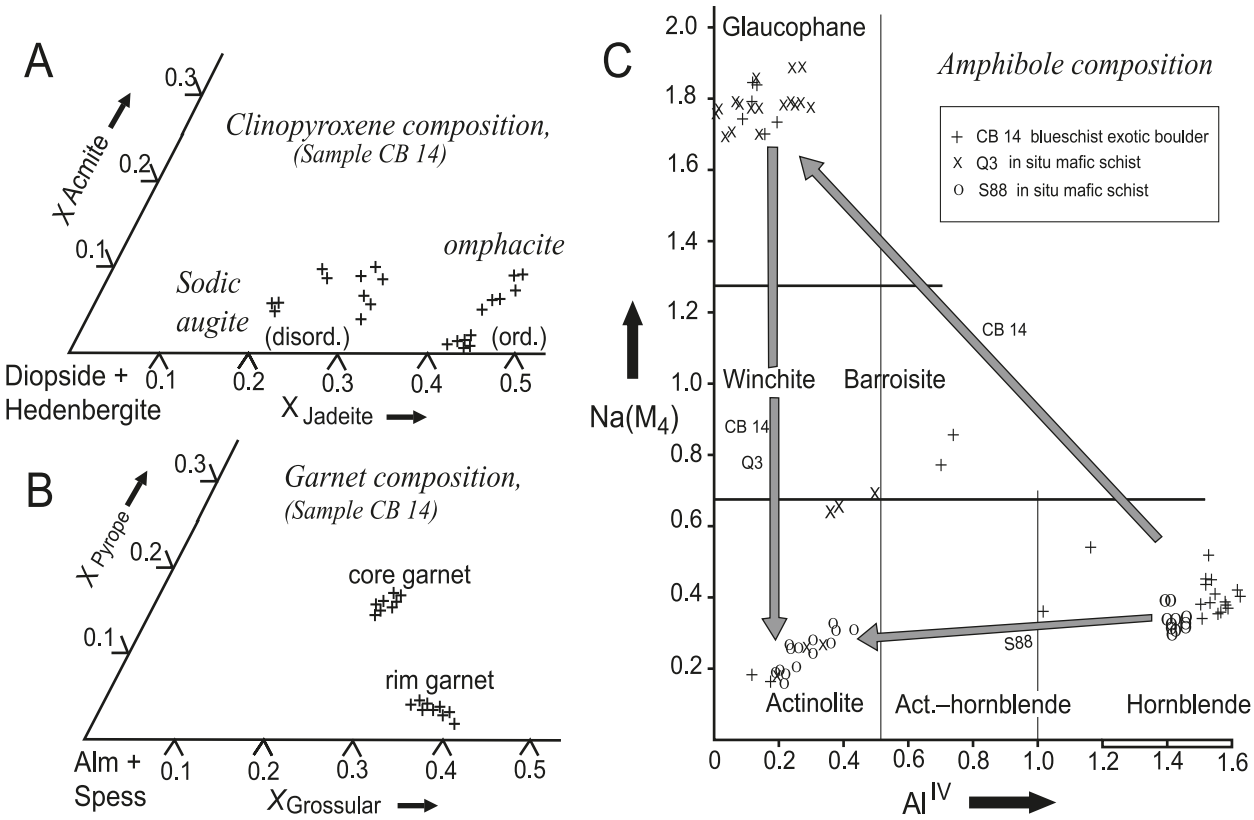

formation of the eclogite. A generalized pseudosection for the exotic Los Pabilos amphibolite boulders generated by Willner et al. (2004) suggests that at an average temperature of 553 °C, the minimum pressure would exceed 1.6 GPa for stability of omphacite bearing assemblages, indicating an even lower geothermal gradient than the maximum gradient suggested here.

The retrograde *P–T* path based on mineral zonation in this sample is consistent with, but at higher pressures than, the composite retrograde path determined for garnet amphibolite exotic boulders considered as the earliest indication of mass underflow along this portion of the Gondwana margin (Willner et al. 2004). However, retro-epidote-amphibolite exotic blocks lacking garnet may have followed a lower retrograde *P–T* path as suggested by Kato and Godoy (1995).

Mineral zonation within the high-grade blueschist–amphibolites suggest a composite counterclockwise *P–T* path (Kato and Godoy 1995; Willner et al. 2004) (See Fig. 6*a*). In the figure, a thick line represents the approximate retrograde path for sample CB14. Thin dashed lines represent published paths for epidote amphibolite (Kato and Godoy 1995) and garnet amphibolite (Willner et al. 2004). The arrows shown for samples Q3 and S88 in Fig. 6*a* are not strictly defined *P–T* "paths" in that the textural relationships observed suggest only *P–T* "displacements" of equilibrium state based on mineral zoning derived from various experimental and calculated equilibria rather than curvilinear paths (Fig. 6*b*).

All of the *P–T* paths shown in Fig. 6*a* suggest a convergence through time of metamorphic grade toward lower greenschist grade conditions indicating a homogenization during decompression and (or) cooling of the complex, which we interpret as the major transpressive exhumational event affecting the Western Series in this area.

^{40}Ar–^{39}Ar dating of high grade blueschist boulders

Ar–Ar age determinations are presented for hornblende and white mica from the coarsely crystalline blueschist (retro-amphibolite) boulders. The dated relict hornblende is from a coarse blueschist (retro-garnet amphibolite). Of the two dated white micas, one is from the same sample as the hornblende, and the other is from a similar block. Both are in textural equilibrium with sodic amphibole

Ar–Ar analytical methods

Purified hornblende and white mica were placed in machined, 1.9 cm diameter Al disks and irradiated with interlaboratory standard Fish Canyon sanidine (FCs, age = 28.02 Ma; Renne et al. 1998; Jourdan and Renne 2007) in the cadmium-shielded, in-core position of the TRIGA-type reactor at Oregon State University. Corrections applied for interfering argon isotopes produced during irradiation are those given by Renne et al. (1998). Neutron fluence for unknowns was determined to ± 0.5% (or better) based on analysis by laser heating of ~36 single grains of FCs, which were closely arrayed on the same level with the unknowns during irradiation. The analytical protocol used for the resistance

Fig. 6. (A) Calculated temperature and pressure for relict eclogite assemblage (star). Inferred *P–T–t*(time) paths for CB14 blueschist (retro-eclogite) exotic boulder, sample Q3 in situ mafic schist with relict crossite, and sample S88 in situ mafic schist with relict hornblende based on mineral zoning. Previous published composite *P–T* paths for epidote amphibolite (Kato and Godoy 1995), for garnet amphibolite (Willner et al. 2001), and for in situ schists at Bahia Mansa (Willner et al. 2004). (B) Various equilibria used to determine *P–T* displacement: (1) Maruyama et al. (1986), (2) Brown (1978), (3) Maresch (1977), (4) Velde (1967), (5) Maruyama et al. (1983), (6) Holland (1983), (7) Banno (1998). Metamorphic facies boundaries are after Spear (1993): ZE, zeolite; PP, prehnite– pumpellyite; GS, greenschist; EA, epidote amphibolite; AM, amphibolite.

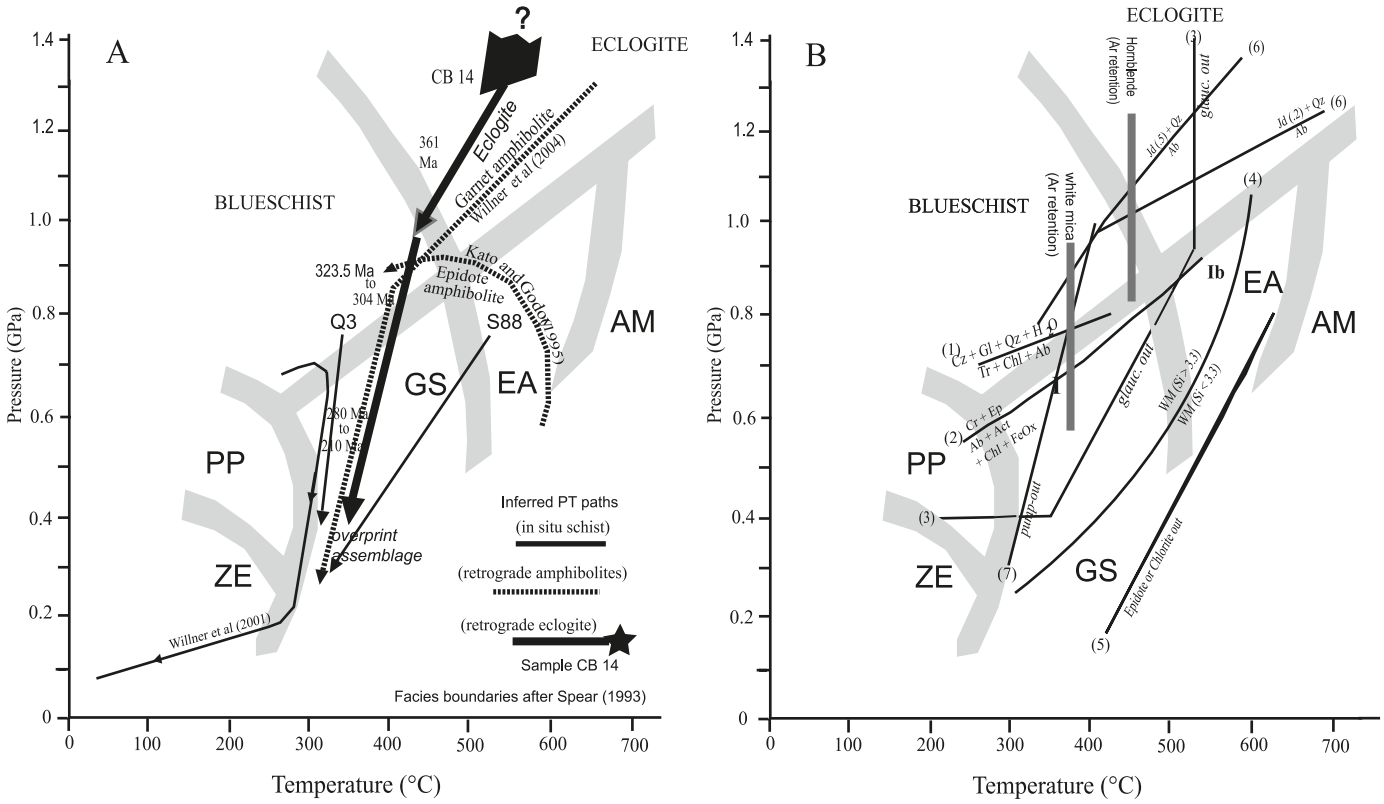

furnace has been described by Sharp et al. (1996). Sample gases were purified by exposure to two SAES GP-50 getters operated at ~450 °C. Argon was analyzed with a Mass Analyzer Products 215-50 mass spectrometer using an electron multiplier operated in analogue mode. The discrimination (mass dependence of spectrometer sensitivity) was determined to be 1.005 ±0.002/amu (atomic mass units) based on ~20 analyses of atmospheric argon admitted from an automated, on-line pipette. Isotopic abundances and decay constants used in age calculations are those of Steiger and Jaeger (1977). Age-errors are quoted at the 95% confidence level.

Hornblende from a garnet-bearing, relict epidote-amphibolite assemblage (sample CB-1) yields a complex age spectrum (Fig. 7*a*). Apparent ages of steps that constitute the first 15% of the cumulative ^{39}Ar released form an asymmetric saddle; that is, the ages monotonically decrease from ~1400 to 210 Ma and then increase to >340 Ma. We interpret the ages for these low-temperature steps in terms of degassing of hornblende containing impurities (most likely white mica) and variable excess ^{40}Ar argon. The first six steps of the age spectrum have Ca/K ratios <4—lower than the Ca/K ratios measured by electron microprobe for nine hornblendes from the coarsely crystalline blocks, which range from 7.2 to 50.1 and have a median value of 12.9. Moreover, as generally observed in polymetamorphic amphibolites (e.g., Ross and Sharp 1988; Dusel-Bacon et al. 2002), CB-1 hornblende contains microscopically visible intergrowths and inclusions of blue amphibole, white mica, sphene, and Fe–Ti oxides that could not entirely be eliminated during purification. Of these, however, only white mica—when present in the low abundance (~1%) observed in sample CB-1—contains enough potassium to reduce the observed calcium/potassium ratio so far below that expected for hornblende. Therefore, we attribute the apparent ages of those steps with low Ca/K ratios (<4), in part, to argon derived from relatively young white mica.

The higher temperature steps of the age spectrum, constituting 15% to 100% of the cumulative ^{39}Ar released, have Ca/K ratios that are higher and relatively constant compared to the earlier steps. Thus, we interpret these steps to be dominated by argon from hornblende. Four of these steps, constituting 62% of the ^{39}Ar released, define a plateau with an age of 361 ± 1.7 Ma. Our estimate of the temperature range for epidote-amphibolite-facies metamorphism (480–680 °C, see earlier in the text) equals or exceeds the likely Ar closure temperature of ~450 ± 50 °C for hornblende (Baldwin et al. 1990). Accordingly, we interpret the age of 361 ± 1.7 Ma as a minimum for epidote-amphibolite metamorphism of the high-grade boulders, and as dating cooling

Fig. 7. Ar–Ar age spectra for (A) relict hornblende in blueschist (retro-garnet amphibolite) CB-1; (B) white mica in textural equilibrium with sodic amphibole in blueschist (retro-garnet amphibolite) CB-1; (C) white mica in textural equilibrium with sodic amphibole in retro-garnet amphibolite CB-18. Exotic boulders from Los Pabilos, Chile (41°S latitude).

along a counterclockwise *P–T* path from the early eclogite–amphibolite phase of metamorphism into blueschist-facies conditions within a thermally maturing subduction zone.

Coarse-grained white mica from sample CB-1 is in textural equilibrium with the sodic amphibole crossite and constitutes part of a blueschist-facies assemblage that partially replaced the epidote-amphibolite assemblage. CB-1 mica yields a spectrum with apparent ages for ~98% of the gas that gently ramp from 320 and 333 Ma (Fig. 7*b*). Steps in the mid- section of this ramp form a plateau with an age of 325 ± 1.1 Ma. The Ar closure temperature of well-crystallized, coarse-grained white mica, about 375 ± 25 °C (e.g., Jager 1979; Hunziker et al. 1992), is comparable to the likely temperature range of crystallization of the blueschist-facies assemblage. Therefore, we interpret the plateau age of CB-1 to approximate the age of blueschist-facies metamorphism of high-grade block CB-1.

Coarse white mica from the blueschist assemblage of another coarse-grained block (sample CB18) yields a similar age spectrum, though it is somewhat more discordant (Fig. 7*c*). The higher temperature steps of this spectrum suggest an age of ≥ 320 Ma for blueschist-facies metamorphism of this block. Steps in the initial 20% of the spectrum yield younger ages that likely reflect reheating or neocrystallization at ≤ 265 Ma, perhaps during regional metamorphism of the Bahía Mansa metamorphic complex (discussed later in the text) that likely formed the matrix for the blocks prior to erosion.

A K–Ar age of 304 ± 9 Ma on white mica (sample S66; analysis by Lanphere, Klock, Saburomaru, and Von Essen, US. Geological Survey) coexisting with sodic amphibole was mentioned in an earlier report (Kato and Godoy 1995). The block was sampled west of Los Pabilos at 40°58′S, 73°34′W. We regard this age as a minimum estimate for blueschist facies metamorphism in light of the discordance observed in the step heating spectra of white micas from the coarse-grained blocks. This date is broadly consistent with a 305.3 ± 3.2 Rb–Sr mineral isochron date on the blueschist metamorphism of these blocks by Willner et al. (2004).

Timing of fluid infiltration and retrograde metamorphism

The data presented suggest that an early phase of medium (epidote amphibolite) to high (eclogite) *P/T* metamorphism (>361 Ma), i.e., Late Devonian (International Commission on Stratigraphy 2004, International Stratigraphic chart 2004) or older, age was followed by Carboniferous (~325 Ma) blueschist (glaucophane + epidote) metamorphic conditions in the anomalous exotic boulders from Los Pabilos. Retrograde passage of the boulders through the hornblende blocking temperature into blueschist-facies conditions defines an increasingly subnormal *P–T* gradient, suggesting that cooling of the newly initiated subduction zone by mass underflow commenced prior to 361 Ma (Late Devonian).

To maintain mass balance, the change in mineralogy from eclogite (garnet + clinopyroxene ± hornblende) or amphibolite (hornblende + plagioclase ± garnet ± epidote) to blueschist (sodic amphibole + epidote + white mica) must have required significant infusion of aqueous fluid into the system. Fluid infiltration studies elsewhere have shown the importance of H_2O fluid influx in the eclogite to garnet glaucophanite transition (Carson et al. 2000). Some of the least retrograded amphibolite samples exhibit fine cataclastic texture at the margin of large hornblende crystals. It is along these zones that incipient glaucophane growth is most evident. Composite zoning relationships from many of the blocks suggest a counterclockwise *P–T* path related to partial subduction and subsequent upward transport of original oceanic crustal fragments, possibly due to serpentinite diapirism (Kato and Godoy 1995; Willner et al. 2004). Willner et al. (2004) suggest a prograde greenschist- to amphibolite-facies gradient of 15 °C/km for the Los Pabilos blueschists; however, only retrograde reactions were observed in our inspection of the Los Pabilos boulders.

Exhumation of blueschists within the Western Series Accretionary Complex

The present position of the older, higher grade blueschist–amphibolite boulders atop the lower grade, more intensely deformed in situ BMMC requires some inversion mechanism. The close association with the distinctive Cuesta Brava serpentinite suggests that the serpentinite may have played a role in emplacing the high-grade blueschists into high levels of the BMMC. Although some of the boulders exhibit incipient greenschist overprint, many of the boulders do not, and may have been emplaced to levels above the lower greenschist level forming the present erosion surface. The timing of ductile deformation and pervasive greenschist overprint metamorphism within the BMMC places constraints on the uplift history of the in situ complex. The clustering of published K–Ar dates on syntectonic white mica suggests that the main deformation and initiation of upward emplacement of the in situ schists occurred between 280 and 245 Ma (Permian – early Triassic) (e.g., Duhart et al. 2001). A U–Pb date on detrital zircon from lower greenschist-grade metasandstone from the BMMC near Bahia Mansa of 265 Ma suggests that much of the complex may consist of younger constituents also affected by the principal Permian–Triassic deformation (Duhart et al. 2001).

Inferred *P–T* paths of the two samples of in situ mafic schist from Los Pabilos showing replacement assemblages are shown as large arrows in Fig. 6*a*. Sample Q3, containing relict crossite replaced by a chlorite–actinolite assemblage (Fig. 3*d*), followed a near-isothermal decompressional path. Sample S88, with relict hornblende, attained higher *T* and may have followed a retrograde exhumational path along a more typical ambient thermal gradient. The relict hornblende in this sample of the in situ BMMC schist is indistinguishable in composition from hornblendes reported in amphibolites from the exotic boulders. Due to the rarity of large relict hornblende in the BMMC mafic schists, we con-

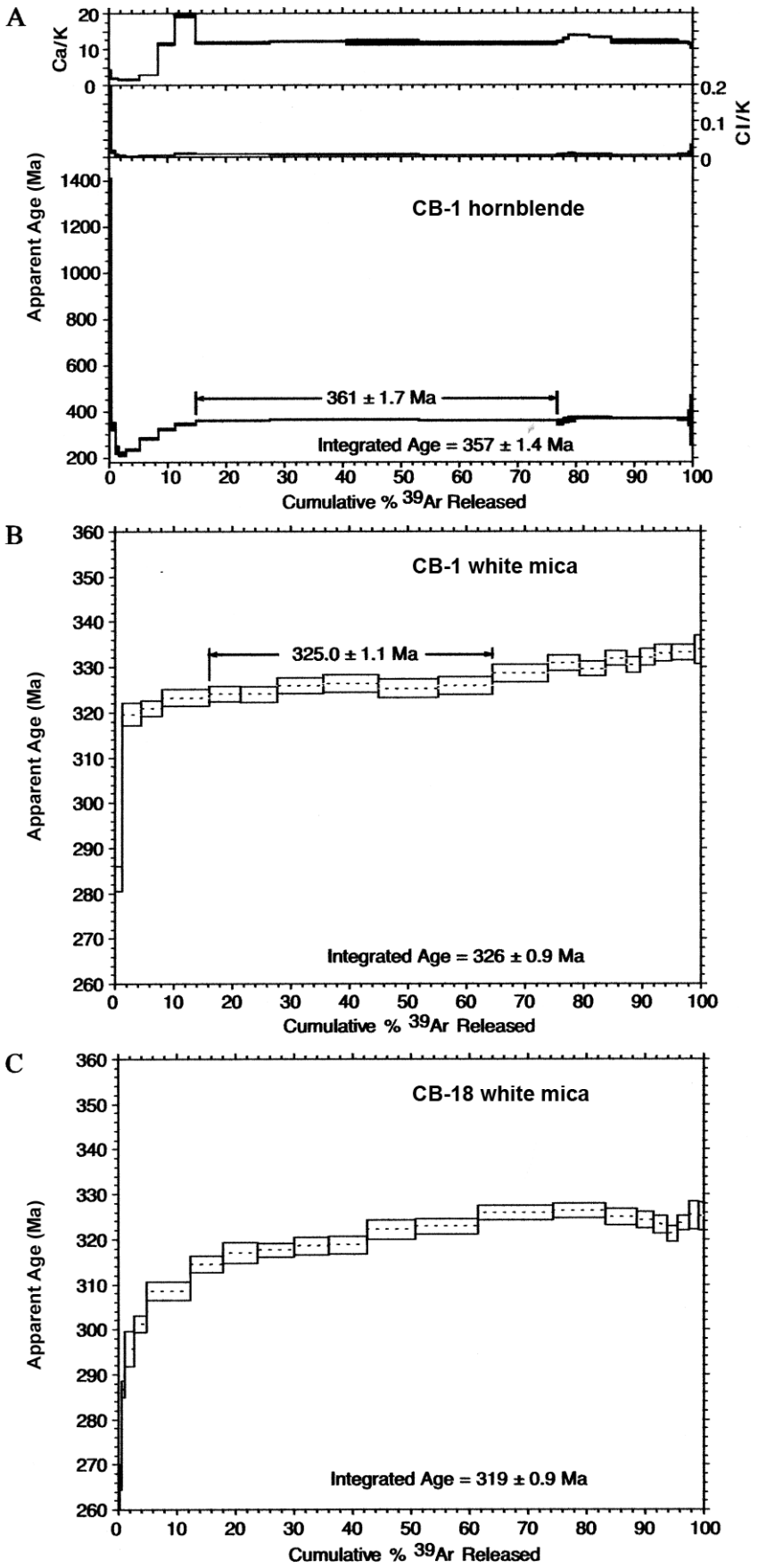

Fig. 8. Conceptual east–west visualization diagram during Permian oblique subduction (transpressive deformation) illustrating exhumation of high-grade blueschist–retroeclogite–amphibolite (B), above in situ schist (MS). Schematic structures represent vertical strain partitioning of D_2 deformation at various structural levels. und., undifferentiated.

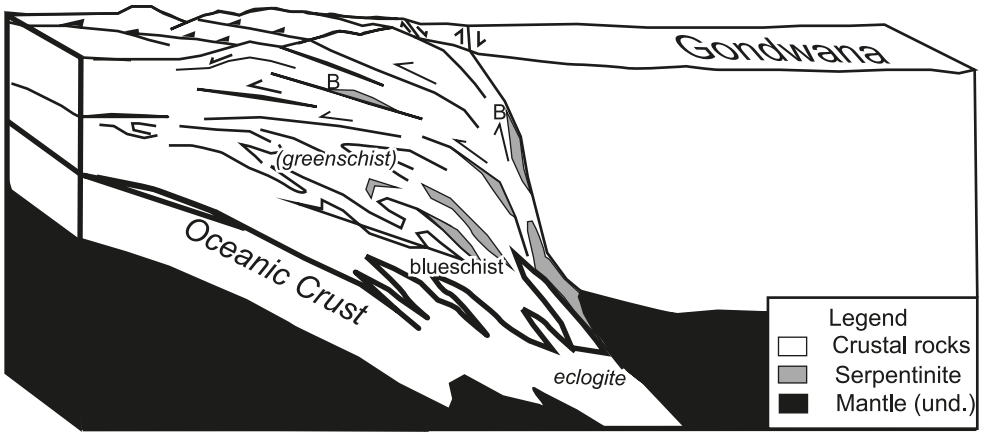

Fig. 9. Schematic evolutionary diagrams showing possible location of Los Pabilos coarse blueschists during the phase of development of the western Gondwana margin beginning with possible collision of post-rift Chilenia with the Precordillera terrane during the Middle Devonian, (Ramos et al. 1986; Davis et al. 1999; Whitmeyer and Simpson 2004) followed by dextral transpression along the Chilean Coast Range and Andean foothills region during the Permian (Martin et al. 1999), coincident with Gondwanide deformation in the North Patagonian Massif of western Argentina (Von Gosen 2003).

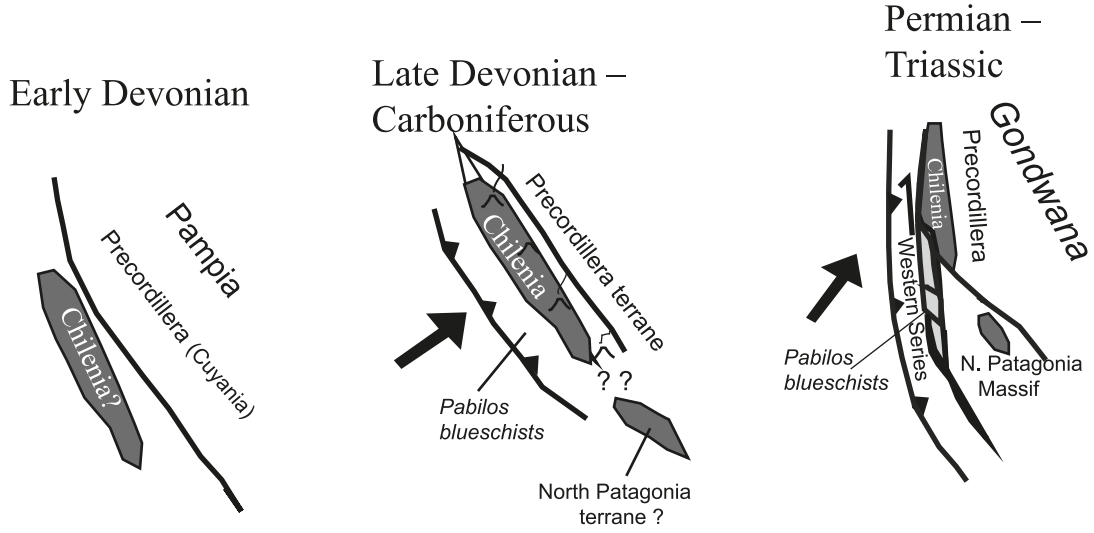

sider amphibolite similar to the exotic blocks to be a volumetrically minor protolith within the predominately younger BMMC.

Most textural features of the BMMC, particularly the dominant S_2 foliation that accompanied the greenschist "overprint" metamorphism on earlier assemblages are thought to be related to upward and lateral nappe emplacement (Kato 1985; Martin et al. 1999). This event is also characterized by ubiquitous syn-folial vein development and retrograde reactions, such as formation of late-stage stilpnomelane (see Fig. 3*c*), suggesting high fluid mobility and fluid pressures during the main D_2 deformational episode (Kato 1985). Figure 8 is a hypothetical scheme for exhumation of the high-grade blocks to higher crustal levels during Permian transpressive deformation of the Western Series subduction complex. The presence of rare relics of high-grade amphibolite (Sample S88) and relict coarse sodic amphiboles (Sample Q3) within the in situ BMMC, similar to the high-grade blueschist–amphibolites, and the incipient growth of actinolite similar to those in the BMMC (Fig. 5*c*) and S_2 foliation (Figs. 6*a*, 6*b*) as greenschist overprint in some of the high-grade boulders provides a tentative link between the exhumation of the high grade blocks and the BMMC.

Tectonic synthesis and regional implications

The high-grade boulders record early eclogite–amphibolite-facies metamorphism followed by cooling and subsequent partial recrystallization under blueschist facies conditions. $^{40}Ar/^{39}Ar$ dating of relict hornblende indicates that eclogite–amphibolite metamorphism took place by ≥361 Ma, and white mica from blueschists yield a plateau age of ~325 Ma. We consider these relations to indicate that the inception of subduction along the western margin of accreted terranes, such as the Chilenia terrane

and Patagonia terranes (Ramos et al. 1986; Davis et al. 1999; Gerbi et al. 2002) may have begun during the Chánic event, which coincides with the end of the Famatinian–Achalian orogenic cycle in the southern Pampean and beginning of the Gondwanide cycle in the northern Patagonia area of South America (Ramos et al. 1986). Based on structural data, Ar–Ar and U–Pb dates and summary of previous radioisotopic work, an age of 384 Ma, or Middle Devonian, has been suggested for the beginning of deformation related to suturing of the Chilenia terrane to the Precordillera terrane near the present location of Mendoza, Argentina, (Davis et al. 1999). Figure 9 is a highly schematic evolutionary diagram based primarily on previous studies intended to relate some of these tectonic events and settings.

The main stage of blueschist metamorphism during the Late Carboniferous, indicated in the Los Pabilos boulders of this study, are thought to correspond with abundant magmatic activity in the North Patagonian batholith exposed in the Coast Range north of 38°S, in the Nahuelbuta Range, and in the Andean foothills to the east of the BMMC (Martin et al. 1999). East of the Andes, in the Argentinian North Patagonian Andean region, although less restricted, magmatic arc activity and crustal remobilization span a larger time interval dating back to the Ordovician (Cingolani et al. 1991; Varela et al. 2005). Some of this earlier magmatism may represent arc activity related to the pre-Late Devonian subduction zone metamorphism. Much of this earlier magmatism is thought to be subduction related, but due to poor preservation or subsequent overprinting, the precise locations of the subduction zones are not well established. The accretion of the North Patagonian Massif (Patagonian terrane) has been suggested during Permo-Triassic Gondwanide deformation (Von Gosen 2003). Detrital zircon evidence from Patagonia suggests, however, that the Patagonia area was autochthonous relative to Gondwana during the Carboniferous (Augustsson et al. 2006).

In summary, we hypothesize that the Late Devonian eclogite–amphibolite to blueschist retrograde metamorphism evidenced in the Los Pabilos exotic boulders developed during initiation of extended late Paleozoic subduction along the paleo-Pacific margin of Gondwana. The input of large volumes of late Paleozoic sediment building up the Western Series (BMMC) forearc accretionary complex and extensive high *P–T* metamorphism may have initiated during the final stages of amalgamation of the southwestern Gondwana continental margin.

Late Paleozoic paleogeographic features in the area have been modified by later offsets along latest Paleozoic – Miocene lateral faults, such as the NW–SE-trending Gastre fault zone in the North Patagonian Massif (Rapela and Pankhurst 1992), transpressional zones in the Chilean Coast Range and Andean Foothills (Kato et al. 1997; Martin et al. 1999) and north–south-trending Liquiñe-Ofqui fault in the Andes (Cembrano et al. 1996). These later faults disrupt the paleogeographic relationships between the earlier terranes throughout large areas of Chile and western Argentina (Godoy 2002). The interpretations presented here support the idea that reactivation and change of character of pre-existing fault zones have greatly modified the Gondwana accretionary margin (Simpson et al. 2001).

Acknowledgements

The authors wish to thank the Servicio Nacional de Geología y Minería de Chile (SERNAGEOMIN) for financial and logistical support provided for this project. M. McDonough, P. Duhart, M. Martin, P. Crigñola, and J. Muñoz provided assistance and insights in the field. J. Wakabayashi, D. Chew, and W. Davis provided helpful reviews. S. Roeske provided technical assistance with the electron microprobe (University of California, Davis, California). S. Roeske and E.H. Brown made helpful suggestions in an early version of the manuscript. G. Yañez provided the grayscale rendition of the Aeromagnetic Map of Chile. W.G. Ernst helped support early field work on this project.

References

Aguirre, L., Hervé, F., and Godoy, E. 1972. Distribution of metamorphic facies in Chile—an outline. Krystalinikum, **9**: 7–19.

Augustsson, C., Münker, C., Bahlburg, H., and Fanning, C.M. 2006. Provenance of late Paleozoic metasediments of the SW South American Gondwana margin: a combined U–Pb and Hf-isotope study of single detrital zircons. Journal of the Geological Society, **163**: 983–995. doi:10.1144/0016-76492005-149.

Bahlburg, H., and Hervé, F. 1997. Geodynamic evolution and tectonostratigraphic terranes of northwestern Argentina and northern Chile. Geological Society of America Bulletin, **109**: 869–884. doi:10.1130/0016-7606(1997)109<0869:GEATTO>2.3.CO;2.

Baldwin, S.L. 1996. Contrasting P–T–t histories for blueschists from the Western Baja terrane and the Aegean: Effects of synsubduction exhumation and backarc extension. *In* Subduction top to bottom. *Edited by* E.G. Bebout, D.W. Scholl, S.H. Kirby, and J.P. Platt. Geophyscial Monograph, 96, pp. 35–141.

Baldwin, S.L., Harrison, T.M., and Fitzgerald, J.D. 1990. Diffusion of ^{40}Ar in metamorphic hornblende. Contributions to Mineralogy and Petrology, **105**: 691–703. doi:10.1007/BF00306534.

Banno, S. 1998. Pumpellyite–actinolite facies of the Sanbagawa metamorphism. Journal of Metamorphic Geology, **16**: 117–128. doi:10.1111/j.1525-1314.1998.00071.x.

Brown, E.H. 1978. A P–T grid for metamorphic index minerals in high pressure terrains. Geological Society of America, Abstracts with Programs, **10**: 373.

Carson, C.J., Clarke, G.L., and Powell, L. 2000. Hydration of eclogite, Pam Peninsula, New Caledonia. Journal of Metamorphic Geology, **18**: 79–90. doi:10.1046/j.1525-1314.2000.00245.x.

Cembrano, J., Hervé, F., and Lavenu, A. 1996. The Liquiñe Ofqui fault zone: a long-lived intra-arc fault system in southern Chile. Tectonophysics, **259**: 55–66. doi:10.1016/0040-1951(95)00066-6.

Cingolani, C., Dalla Salda, L., Hervé, F., Munizaga, F., Pankhurst, R.J., Parada, M.A., and Rapela, C.W. 1991. The magmatic evolution of northern Patagonia; new impressions of pre-Andean and Andean tectonics. *In* Andean magmatism and its tectonic setting. *Edited by* R.S. Harmon and C.W. Rapela. Geological Society of America, Special Paper 265, pp. 29–44.

Cloos, M. 1986. Blueschists in the Franciscan subduction Complex of California. *In* Petrotectonic constraints on uplift mechanisms. *Edited by* B.W. Evans and E.H. Brown. Geological Society of America, Memoir 164, pp. 77–94.

Coleman, R.G., and Lee, D.E. 1963. Glaucophane bearing metamorphic rock types of the Cazadero area, California. Journal of Petrology, **4**: 260–301.

Davis, J.S., Roeske, S.M., McClelland, W.C., and Snee, L.W. 1999. Closing the ocean between the Precordillera terrane and Chilenia: Early Devonian ophiolite emplacement and deformation in the southwest Precordillera. *In* Laurentia–Gondwana connections

before Pangea. *Edited* by V.A. Ramos and J.D. Keppie. Geological Society of America, Special Paper 336, pp. 115–138.

Duhart, P., McDonough, M., Muñoz, J., Martin, M.W., and Villenueve, M. 2001. El Complejo Bahía Mansa en la Cordillera de la Costa del centro-sur de Chile (39°30′ –42°00′S). Revista Geológica de Chile, **28**: 179–208.

Dusel-Bacon, C., Lanphere, M.A., Sharp, W.D., Layer, P.W., and Hansen, V.L. 2002. Mesozoic thermal history and timing of structural events for the Yukon–Tanana Upland, east-central Alaska: $^{40}Ar/^{39}Ar$ data from metamorphic and plutonic rocks. Canadian Journal of Earth Sciences, **39**: 1013–1051. doi:10.1139/e02-018.

Ernst, W.G. 1975. Systematics of large-scale tectonics and age progressions in Alpine and Circum-Pacific blueschist belts. Tectonophysics, **26**: 229–246. doi:10.1016/0040-1951(75)90092-X.

Ernst, W.G., Seki, Y., Onuki, H., and Gilbert, M.C. 1970. Comparative study of low grade metamorphism in the California Coast Range and the outer metamorphic belt of Japan. Geological Society of America, Memoir 124.

Fortey, R., Pankhurst, R.J., and Hervé, F. 1992. Devonian Trilobites at Buill, Chile (42°S). Revista Geológica de Chile, **19**: 133–144.

Gerbi, C., Roeske, S.M., and Davis, J.S. 2002. Geology and structural history of the southwest Precordillera margin, northern Mendoza Province, Argentina. Journal of South American Earth Sciences, **14**: 821–835. doi:10.1016/S0895-9811(01)00080-3.

Ghent, E.D. 1988. A review of chemical zoning in eclogite garnets, *In* Eclogites and eclogite facies rocks. *Edited by* Smith, D.C. Elsevier, Amsterdam, The Netherlands, pp. 207–236.

Godoy, E. 2002. Dominios tectónicos pérmicos-mesozoicos en el centro y sur de Chile y Argentina. *In* Actas del XV Congreso Geológico Argentina, 1, pp. 155–160.

Godoy, E., and Kato, T. 1990. Late Paleozoic serpentinites and mafic schists from the Coast Range accretionary complex, central Chile: their relation to aeromagnetic anomalies. Geologische Rundschau, **79**: 121–130. doi:10.1007/BF01830451.

Godoy, E., Hervé, F., Mpodozis, C., and Davidson, J. 1984. Deformación polifásica y metamorfismo progresivo en el basamento de Archipelago de Chonos; Aysén, Chile. *In* Actas IX Congreso Geologico Argentino, Bariloche, 4, pp. 211–232.

González-Bonorino, F. 1970. Metamorphism of the crystalline basement of central Chile. Journal of Petrology, **59**: 979–993.

Hervé, F., Munizaga, F., Godoy, E., and Aguirre, L. 1974. Late Paleozoic K/Ar ages of blueschists from Pichilemu, central Chile. Earth and Planetary Science Letters, **23**: 261–264. doi:10.1016/0012-821X(74)90200-3.

Hervé, F., Davidson, D., Godoy, E., Mpodozis, C., and Corvacevich, V. 1981. The late Paleozoic in Chile: Stratigraphy, structure, and possible tectonic framework. Anais da Academia Brasileira de Ciencias, **53**: 361–373.

Hervé, F., Munizaga, F., Parada, M.A., Brook, M., Pankhurst, R.J., Snelling, N.J., and Drake, R. 1988. Granitoids of the Coast Range of Central Chile: Geochronology and geological setting. Journal of South American Earth Sciences, **1**: 185–192. doi:10.1016/0895-9811(88)90036-3.

Holland, T.J.B. 1983. The experimental determination of activities in disordered and short-range ordered jadeitic pyroxenes. Contributions to Mineralogy and Petrology, **82**: 214–220. doi:10.1007/BF01166616.

Hunziker, J.C., Desmons, J., and Hurford, A.J. 1992. Thirty-two years of geochronological research in the Central and Western Alps: a review on seven maps. Mémoires de Geologie (Lausanne), Vol. 13, pp. 1–59.

International Commission on Stratigraphy. 2004. International Stratigraphic Chart. International Union of Geological Sciences. International Commission on Stratigraphy, Paris, France.

Jager, E. 1979. Introduction to Geochronology. *In* Lectures in isotope geology. *Edited by* E. Jager and J.C. Hunziker. Springer-Verlag, Berlin, pp. 1–12.

Jourdan, F., and Renne, P.R. 2007. Age calibration of the Fish Canyon sanidine $^{40}Ar/^{39}Ar$ dating standard using primary K–Ar standards. Geochimica et Cosmochimica Acta, **71**: 387–402. doi:10.1016/j.gca.2006.09.002.

Kato, T.T. 1976. The relationship between low-grade metamorphism and tectonics in the Coast Ranges of central Chile. Unpublished Ph.D. thesis, University of California, Los Angeles, Calif., 120 p.

Kato, T.T. 1985. Pre-Andean orogenesis in the Coast Ranges of central Chile. Geological Society of America Bulletin, **96**: 918–924. doi:10.1130/0016-7606(1985)96<918:POITCR>2.0.CO;2.

Kato, T.T., and Godoy, E. 1995. Petrogenesis and Tectonic Significance of Late Paleozoic Coarse-Crystalline Blueschist and Amphibolite Boulders in the Coastal Range of Chile. International Geology Review, **37**: 992–1006.

Kato, T.T., Godoy, E., McDonough, M., Duhart, P., Martin, M., and Sharp, W. 1997. Un modelo preliminar de deformación transpresional Mesozoica y gran desplazamiento hacia el Norte de parte de la Serie Occidental, Complejo Acrecionario (38°S a 43°S), Cordillera de la Costa, Chile. *In* Congreso Geológico Chileno, Antofagasta. Vol. 1, pp. 98–102.

Krogh Ravna, E.K. 2000. The garnet–clinopyroxene Fe^{2+} –Mg geothermometer: an updated calibration. Journal of Metamorphic Geology, **18**: 211–219. doi:10.1046/j.1525-1314.2000.00247.x.

Maresch, W.V. 1977. Experimental studies on glaucophane: An analysis of present knowledge. Tectonophysics, **43**: 109–125. doi:10.1016/0040-1951(77)90008-7.

Martin, M.W., Kato, T.T., Rodriguez, C., Godoy, E., Duhart, P., McDonough, M., and Campos, A. 1999. Evolution of late Paleozoic accretionary complex and overlying forearc – magmatic arc, South-central Chile (38°–41°S): Constraints for the tectonic setting along the southwestern margin of Gondwana. Tectonics, **18**: 582–605. doi:10.1029/1999TC900021.

Maruyama, S., Suzuki, K., and Liou, J.G. 1983. Greenschist–amphibolite transition equilibria at low pressures. Journal of Petrology, **24**: 583–604.

Massonne, H.J., Medenbach, O., Willner, A., et al. 1998. Zussmanite in the late Paleozoic metamorphic complex of Southern Chile. Mineralogical Magazine, **62**: 869–876. doi:10.1180/002646198548098.

Mpodozis, C., and Kay, S.M. 1992. Late Paleozoic to Triassic evolution of the Gondwana margin: Evidence from the Chilean Frontal Cordillera batholith (28°S to 28°S. Geological Society of America Bulletin, **104**: 999–1014. doi:10.1130/0016-7606(1992)104<0999:LPTTEO>2.3.CO;2.

Papike, J.J., Cameron, K.L., and Baldwin, K. 1974. Amphiboles and pyroxenes: Characterization of other than quadrilateral components and estimates of ferric iron from microprobe data. Geological Society of America, Abstracts with Programs, **6**: 1053–1054.

Ramos, V.A., Jordan, T.E., Allmendinger, R.W., Mpodozis, C., Kay, S.M., Cortés, J.M., and Palma, M. 1986. Paleozoic terranes of the central Argentine–Chilean Andes. Tectonics, **5**: 855–880. doi:10.1029/TC005i006p00855.

Rapela, C.W., and Pankhurst, R.J. 1992. The granites of northern Patagonia and the Gastre Fault System in relation to the breakup of Gondwana. *In* Magmatism and the causes of continental break-up. *Edited by* B.C. Storey, T. Alabaster, and R.J. Pankhurst. Geological Society, Special Publication, 68, pp. 209–220.

Renne, P.R., Swisher, C., Deino, A.L., Karner, B.D., Owens, T.L., and DePaolo, D.L. 1998. Intercalibration of standards, absolute ages and uncertainties in $^{40}Ar/^{39}Ar$ dating. Chemical Geology, **145**: 117–152. doi:10.1016/S0009-2541(97)00159-9.

Ross, J.A., and Sharp, W.D. 1988. The effects of sub-blocking temperature metamorphism on the K–Ar systematics of hornblendes: $^{40}Ar/^{39}Ar$ dating of polymetamorphic garnet amphibolite from the Franciscan Complex, California. Contributions to Mineralogy and Petrology, **100**: 213–221. doi:10.1007/BF00373587.

Rossi, G. 1988. A review of the crystal-chemistry of clinopyroxenes in eclogites and other high-pressure rocks. *In* Eclogites and eclogite facies rocks. *Edited by* D.C. Smith. Elsevier, Amsterdam, The Netherlands, pp. 237–270.

Saliot, P.1969. Étude géologique dans l'île de Chiloé (Chili). Bulletin de la Société Geologique de France, Série 7, **11**: 388–399.

Sharp, W.D., Turrin, B.D., Renne, P.R., and Lanphere, M.A. 1996. $^{40}Ar/^{39}Ar$ and K–Ar dating of lavas from the Hilo 1-km corehole, Hawaii Scientific Drilling Project. Journal of Geophysical Research, **101**: 11 607–11 616. doi:10.1029/95JB03702.

Simpson, C., Whitmeyer, S.J., De Paor, D.G., Gromet, L.P., Miro, R., Krol, M.A., and Short, H. 2001. Sequential ductile through brittle reactivation of major fault zones along the accretionary margin of Gondwana in Central Argentina. *In* The nature and tectonic significance of fault zone weakening. *Edited by* R. Holdsworth et al. Geological Society (of London), Special Publications 186, pp. 233–255.

Spear, F.S. 1993. Metamorphic Phase Equilibria and Pressure–Temperature–Time Paths. Mineralogical Society of America, Monograph Series, Washington D.C., 799 p.

Steiger, R.H., and Jaeger, E. 1977. Subcommission on geochronology: Convention on the use of decay constants in geo- and cosmochronology. Earth and Planetary Science Letters, **36**: 359–362. doi:10.1016/0012-821X(77)90060-7.

Tsujimori, T., Matsumoto, K., Wakabayashi, J., and Liou, J.G. 2006. Franciscan eclogite revisited: reevaluation of P–T evolution of tectonic blocas from Tiburon Peninsula, California. Contributions to Mineralogy and Petrology, **88**: 243–267.

Varela, R., Basei, M.A.S., Cingolani, C.A., Siga, O., Jr., and Passarelli, C.R. 2005. El basamento cristalino de los Andes Nordpatagónicos en Argentina: geocronología e interpretación tectónica. Revistas Geológica de Chile, **32**: 167–188.

Velde, B. 1967. Si^{+4} content of natural phengites. Contributions to Mineralogy and Petrology, **14**: 250–258. doi:10.1007/BF00376643.

Von Gosen, W. 2003. Thrust tectonics in the North Patagonian Massif (Argentina): Implications for a Patagonia plate. Tectonics, **22**: 5-1–5-33.

Wakabayashi, J. 1990. Counterclockwise P–T–t paths from amphibolites, Franciscan Complex; California: Metamorphism during the early stages of subduction. The Journal of Geology, **98**: 657–680.

Whitmeyer, S.J., and Simpson, C. 2004. Regional deformation of the Sierra de San Luis, Argentina: Implications for the Paleozoic development of Western Gondwana. Tectonics, **23**: TC1005, 16 p.

Willner, A.P., Hervé, F., and Massone, H. 2000. Mineral chemistry and Pressure–Temperature Evolution of Two Contrasting High pressure – Low temperature belts in the Chonos Archipelago, Southern Chile. Journal of Petrology, **41**: 309–330. doi:10.1093/petrology/41.3.309.

Willner, A., Pawlig, S., Massonne, H., and Hervé, F. 2001. Metamorphic evolution of spessartine quartzites (coticules) in the high-pressure, low temperature complex at Bahia Mansa, Coastal Cordillera of south-central Chile. Canadian Mineralogist, **39**: 1547–1569. doi:10.2113/gscanmin.39.6.1547.

Willner, A.P., Glodny, J., Gerya, T.V., Godoy, E., and Massonne, H.J. 2004. A counterclockwise PT path of high-pressure/low temperature rocks from the Coastal Cordillera accretionary complex of south-central Chile: constraints for the earliest stage of subduction mass flow. Lithos, **75**: 283–310. doi:10.1016/j.lithos.2004.03.002.